2020 IEEE International Conference on Robotics and Automation (ICRA)
31 May - 31 August, 2020. Paris, France

# Avalanche victim search via robust observers

Nicola Mimmo, Pauline Bernard and Lorenzo Marconi

*Abstract*— **This paper introduces a new approach for victim localization in avalanches that will be exploited by UAVs using the ARVA sensor. We show that the nominal ARVA measurement can be linearly related to a quantity that is sufficient to reconstruct the victim position. We explicitly deal with a robust scenario in which the measurement is actually perturbed by a noise that grows with the distance to the victim and we propose an adaptive control scheme made of a least-square identifier and a trajectory generator whose role is both to guarantee the persistence of excitation for the identifier and to steer the ARVA receiver towards the victim. We show that the system succeeds in localizing the victim in a domain where the ARVA output is sufficiently informative and illustrate its performance in simulation. This new approach could significantly reduce the searching time by providing an exploitable estimate before having reached the victim. The work is framed within the EU project AirBorne whose goals is to develop at TRL8 a drone for quick localization of victims in avalanche scenarios.**

Search and Rescue, Robust Control

## I. Introduction

The system ARVA consists of two elements: a *transmitter* and a *receiver*. The transmitter is worn by the victim and emits an electromagnetic signal detectable by the receiver, which is held by the rescuers. In case of signal detection, the receiver provides information about the electromagnetic field generated by the transmitter sensed at the receiver device location. The rescuers are trained to interpret these data and to move closer to the victim location. Unfortunately, although this technique is common and quite efficient, it requires a non negligible amount of time due to the difficulties in walking in avalanche terrains. Furthermore, the rescuers walk on unstable snow with the tangible risk of inducing a second avalanche event. In this context, drones represent a valid alternative to humans. Indeed, if sufficiently smart, ARVA-driven drones can fly autonomously to find the transmitter location thus resulting in faster and safer search. Related to alpine environment, [1], [2], [3] demonstrated how S&R operations can greatly benefit from the use of autonomous UAVs to survey the environment and collect evidence about the position of a missing person. Furthermore, the European projects *SHERPA* [4] and *AIRBorne* [5] address a specific challenge in S&R robotics, *i.e.* the establishment of an effective solution to support professional alpine rescuer teams in avalanches scenarios. AirBorne, in particular, deals with developing at TRL8 an ARVA drone for quick localization of avalanche victims.

There are two main general approaches in finding the transmitter location. The first one requires the receiver to move closer to the transmitter to minimize the relative distance, whereas the second one is based on an estimation of the transmitter location, without necessary making the receiver approach the transmitter. The current rescue techniques, along with all the available examples of UAVs equipped with the ARVA technology, belong to the first category [6], [7], [8]. In fact, those methods belong to the so-called *source seeking* control problems, where the agent (or agents in case of collaborative and distributed scenarios) senses the signal emitted by a source located at an unknown position and is steered towards it. Remarkable examples include [9], [10], [11] in which the *extremum seeking* control paradigm has been exploited to provide the solution in absence of both a detailed output map and information about the agent's position. Similar methods appear also in [12], [13].

Unlike earlier approaches, this paper presents an algorithm which estimates the victim location by following a trajectory that is sufficiently "rich" in ARVA data. Our first contribution is to show that the ARVA output can be approximated by an output that is linear in a quantity enabling to reconstruct the victim position. It follows that the latter can be estimated by means of a least-square algorithm if the receiver's trajectory is *sufficiently exciting* [14]. A distinguishing feature of our work is that we explicitly take into account the noise corrupting the ARVA signal whose magnitude grows with the relative distance between the transmitter and the receiver. A reference trajectory generator is thus designed to serve a triple purpose: 1) ensuring boundedness of the drone's trajectory 2) guaranteeing persistence of excitation for estimation of the victim position 3) bringing the receiver closer to the victim to limit the noise and improve the estimation. By adopting common terminologies, the approach we follow in this paper falls into the *adaptive control* category and more specifically in the class of the *indirect adaptive control* in which the plant parameters (in particular the victim's position) are estimated on-line and used to calculate the controller parameters [14]. In this class of problems, the control law cannot be designed independently from the identification scheme. Rather it must accomplish the double role of sufficiently exciting the system to make it sufficiently informative for identification purposes and to use the resulting identification outcome to move closer to the victim [15], [16], [17], [18]. We show that there exists a region where the ARVA is sufficiently informative to guarantee convergence to a ball around the victim, whose

P. Bernard is with the Systems and Control Centre of MINES ParisTech, Université PSL, 60 Boulevard Saint-Michel, 75006 - Paris, France. e-mail: pauline.bernard@mines-paristech.fr.

N. Mimmo and L. Marconi are with the Department of Electrical, Electronic and Information Engineering, University of Bologna, Italy, Viale del Risorgimento 2, 40136 - Bologna (BO). e-mail: {nicola.mimmo2, lorenzo.marconi} @unibo.it.

This research was supported by the European Project "AerIal RoBotic technologies for professiOnal seaRch aNd rescuE" (AirBorne), Call: H2020, ICT-25-2016/17, Grant Agreement no: 780960.

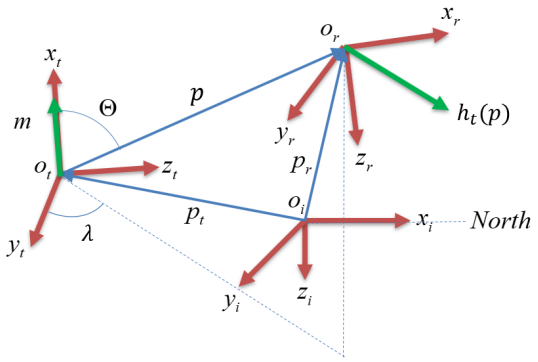


Fig. 1: Reference frames definition

radius depends on the amplitude of the excitation signal. The advantage of this approach is that it provides an exploitable estimate of the victim position before having actually reached it. Those performances are illustrated on simulations.

This paper is organized as follows: Section II introduces the notations, then Section III describes the ARVA system and Section IV the blocks constituting the control scheme (*i.e.* the identifier and the reference trajectory generator) while the main theorem is presented in Section V. Finally, Section VI illustrates the performance of our adaptive control in simulations.

## II. Notations

By $\|\cdot\|$ we denote the standard Euclidean norm and $\|f\|_{t_0,t} = \sup_{s\in[t_0,t]}\|f(s)\|$ for $t \geq t_0 \geq 0$. A function $\gamma : \mathbb{R}_{\geq 0} \to \mathbb{R}_{\geq 0}$ is said to be class-$\mathcal{K}$ if $\gamma(0) = 0$ and $\gamma$ is strictly increasing. A function $\beta : \mathbb{R}_{\geq 0} \times \mathbb{R}_{\geq 0} \to \mathbb{R}_{\geq 0}$ is said to be class-$\mathcal{KL}$ if for every $s \in \mathbb{R}_{\geq 0}$, $r \mapsto \beta(r, s)$ is class-$\mathcal{K}$ and for every $r \in \mathbb{R}_{\geq 0}$, $s \mapsto \beta(r, s)$ is decreasing and $\lim_{s\to+\infty}\beta(r, s) = 0$. $\mathcal{B}_\rho(x)$ denotes the ball of radius $\rho$ centered at $x$. Three Cartesian coordinate frames are defined (see Figure 1): $\mathcal{F}_i = (\mathrm{O}_i, \mathrm{x}_i, \mathrm{y}_i, \mathrm{z}_i)$ indicates the inertial frame with origin $\mathrm{O}_i$, with the unitary vector $\mathrm{x}_i$ oriented toward geographic north, $\mathrm{z}_i$ oriented opposite to the local gravity vector and $\mathrm{y}_i$ oriented to create a right hand frame, while $\mathcal{F}_t = (O_t, \mathrm{x}_t, \mathrm{y}_t, \mathrm{z}_t)$ and $\mathcal{F}_r = (\mathrm{O}_r, \mathrm{x}_r, \mathrm{y}_r, \mathrm{z}_r)$ are the body right hand frames associated respectively to the transmitter worn by the victim and to the receiver installed on the drone. For simplicity sake, we assume that the body frame of the drone coincides with $\mathcal{F}_r$. The position of $\mathrm{O}_r$ relative to $\mathrm{O}_t$ is indicated by the vector $p \in \mathbb{R}^3$, with $p = p_r - p_t$, while the positions of $\mathrm{O}_r$ and $\mathrm{O}_t$ relative to $\mathrm{O}_i$ are indicated respectively by the vectors $p_r \in \mathbb{R}^3$ and $p_t \in \mathbb{R}^3$. Throughout the paper, and only when needed, we shall use the apex $i$, $t$ and $r$ on the left of the vectors $p$, $p_t$, $p_r$ to denote the representation of the previous vectors in the reference frames $\mathcal{F}_i$, $\mathcal{F}_t$ and $\mathcal{F}_r$ respectively (for instance, ${}^i p$ denotes a representation of $p$ in $\mathcal{F}_i$). The quantities are intended in the inertial frame $\mathcal{F}_i$ when the left side apex in not indicated. The rotation matrices from $\mathcal{F}_i$ to $\mathcal{F}_t$ and from $\mathcal{F}_r$ to $\mathcal{F}_i$ are respectively denoted by $R_t$ and $R_r$ whereas the relative rotation from $\mathcal{F}_t$ to $\mathcal{F}_r$ is indicated by $R_{rt}$.

**Definition 1** (Persistence of Excitation). *[14] Given $T > 0$, a locally integrable function $\phi : \mathbb{R}_{>0} \mapsto \mathbb{R}^n$ is said to be **persistently exciting** if there exists a positive real $\alpha_0 > 0$ such that*

$$\frac{1}{T}\int_{t-T}^{t}\phi(\tau)\phi^\top(\tau)\,d\tau \geq \alpha_0 I \qquad \forall t \geq T. \tag{1}$$

## III. Characterisation of the ARVA system

The ARVA system is based on the emission and sensing of an electromagnetic field. More precisely, the transmitter, worn by the victim, emits a signal which is sensed, elaborated and made available to the rescuer by the receiver. In this section, we go through the main features of the sensor that are instrumental for the development of the automatic search algorithms presented in Section V.

### A. ARVA in the transmitter mode

The ARVA system relies on a transmitter device that generates a magnetic field modelled as a dipole aligned with the $\mathrm{x}_t$ axis of $\mathcal{F}_t$ with an amplitude $m \in \mathbb{R}_{>0}$. The electromagnetic vector field, described in $\mathcal{F}_t$, is indicated by $h_t \in \mathbb{R}^3$. Denoting $(x, y, z)$ the components of the vector $p$ expressed in $\mathcal{F}_t$ (i.e. ${}^t p = \mathrm{col}(x, y, z)$), a mathematical model of the magnetic vector field at ${}^t p$ is given by (see [19])

$$h_t(\|p\|, \Theta, \lambda) = \frac{m}{4\pi\|p\|^3}\mathrm{A}_p(\Theta, \lambda) \tag{2}$$

$$\text{where } \mathrm{A}_p(\Theta, \lambda) = \begin{bmatrix} 2 - 3\sin^2\Theta \\ 3\cos\Theta\sin\Theta\cos\lambda \\ 3\cos\Theta\sin\Theta\sin\lambda \end{bmatrix} \text{ and}$$

$$\begin{bmatrix} \Theta \\ \lambda \\ \|p\| \end{bmatrix} = \begin{bmatrix} \cos^{-1}\left(\dfrac{x}{\sqrt{x^2+y^2+z^2}}\right) \\ \tan^{-1}\left(\dfrac{z}{y}\right) \\ \sqrt{x^2+y^2+z^2} \end{bmatrix}. \tag{3}$$

The intensity of the magnetic field is then obtained from the previous relation (see [19]):

$$\|h_t\| = \frac{m}{4\pi\|p\|^3}\sqrt{1 + 3\cos^2\Theta}\,. \tag{4}$$

### B. ARVA in the receiver mode

The ARVA equipment has three antennas directed along the receiver frame axes $\mathrm{x}_r$, $\mathrm{y}_r$ and $\mathrm{z}_r$, namely along the longitudinal, lateral and vertical direction of the sensor case. We assume that the ARVA receiver position $p_r$ and orientation $R_r$ in the inertial frame are known.

The magnetic field read by the receiver, denoted by $h_m(p, R_{rt}, t)$, is given by the projection of the vector $h_t$ onto the $\mathcal{F}_r$ frame corrupted by the sensor noise

$$h_m(p, R_{rt}, t) = R_{rt}h_t({}^t p) + {}^r w(t) \tag{5}$$

where ${}^r w(t) : \mathbb{R} \mapsto \mathbb{R}^3$ indicates the Electro-Magnetic Interference (EMI) expressed in the receiver frame. This noise is bounded by a positive constant $\|{}^r w\|_\infty$. We will denote $h_n(p, R_{rt}) = R_{rt}h_t({}^t p)$ the nominal EM field at the receiver, equal to $h_m(p, R_{rt}, t)$ in absence of noise.

In the following, we would like to exploit this ARVA output (5) to estimate the transmitter's position $p_t$, namely the victim's position, by means of the design of an observer. The estimation of its orientation $R_t$ on the other hand is not crucial and is left aside in this paper.

*a) Toward the transmitter position estimation:* The direct design of a non-linear observer for this system is not straightforward unless adopting an extended Kalman filter [20], which, however, would require linearizing the system and would ensure only a local convergence. On the other hand, the constant nature of the unknowns, namely the position and orientation of the victim, can be exploited for the design of an observer with more appealing properties (easy design, global stability, etc.). In this context, we manipulate the non-linear map $h_n(p, R_{rt})$ to find a change of unknowns that makes the output map linear, thus leading to a simpler observer design. In other words, we design an observer by *immersion*, *i.e.* by immersing (in the differential geometry sense) the state space into a space of larger dimension [21].

More precisely, computations on $h_n$ show that $p$, $R_t$ and $h_n$ fulfill a polynomial equation of the form

$$p^\top M p - (4\pi)^2 \|h_n\|^2 \left(p^\top p\right)^4 = 0 \tag{6}$$

in which $e_1 = \mathrm{col}(1,0,0)$ and $M = M^\top = m^2\left(3R_t e_1 e_1^\top R_t^\top + I\right)$. The equation (6) is a polynomial of degree 8 in the unknown constants $p_t \in \mathbb{R}^3$ and $M \in \mathbb{R}^{3\times 3}$ with coefficients depending on $p_r$ and $h_n$ that are known, modulo some noise on $h_n$. It could therefore be used as an implicit output map to estimate $p_t$ and $M$ (9 unknowns) by an immersion in a linear space of order 54, but this method is practically unfeasible. Instead, we show that a model approximation enables to reduce the dimension and leads to a more practical solution.

*b) ARVA Model approximation:* A detailed analysis of (4) reveals that the complexity is introduced by the term $\sqrt{1+3\cos^2\Theta}$. So the idea is to approximate this function with an equivalent one, namely $f_{\text{eq}}(\Theta)$, which belongs to the family of functions which are isomorphic to $\sqrt{1+3\cos^2\Theta}$ but make (4) inversely proportional to a polynomial of $p$. This paper adopts this approximation

$$\frac{1}{\sqrt[3]{1+3\cos^2\Theta}} \approx \frac{1}{a^2}\cos^2\Theta + \frac{1}{b^2}\sin^2\Theta. \tag{7}$$

**Remark 1.** *The selection of this function is motivated by the fact that the iso-power surface of the electromagnetic field of* (2) *look like ellipsoids, which are $x_t$-axial symmetric, and whose shape is defined by $a$, $b \in \mathbb{R}_{>0}$. Those coefficients $a$ and $b$ are known and chosen to minimize the quadratic error with respect to* $(1+3\cos^2\Theta)^{-1/3}$.

Given the approximation of (7) and keeping in mind (3), the norm of $h_n$ becomes

$$\|h_n\| \approx \frac{m}{4\pi}\left(\frac{a^2b^2}{b^2x^2 + a^2(y^2+z^2)}\right)^{\frac{3}{2}} \tag{8}$$

which, after some manipulations, leads to

$$\left(\frac{m}{\|h_n\|4\pi}\right)^{\frac{2}{3}}(ab)^2 = (p_r - p_t)^\top \overline{M}\,(p_r - p_t) \tag{9}$$

where $\overline{M} = \overline{M}^\top > 0$ with

$$\overline{M} = R_t\,\mathrm{diag}(b^2, a^2, a^2)R_t^\top. \tag{10}$$

(9) can then be rearranged into the linear relation

$$\eta = \Phi^\top(p_r)\,\mathrm{x}(x_t) \tag{11}$$

in which

$$\eta = \left(\frac{m}{\|h_n\|4\pi}\right)^{\frac{2}{3}}(ab)^2 \tag{12}$$

$$\begin{aligned}\Phi^\top(p_r) = [&x_r^2 \quad 2x_ry_r \quad 2x_rz_r \quad y_r^2 \quad 2y_rz_r \quad \dots\\ &\dots \quad z_r^2 \quad -2x_r \quad -2y_r \quad -2z_r \quad 1]\end{aligned} \tag{13}$$

are known signals and

$$\mathrm{x}(x_t) = \mathrm{col}(\overline{m}_{11}, \overline{m}_{12}, \overline{m}_{13}, \overline{m}_{22}, \overline{m}_{23}, \overline{m}_{33}, \overline{p}_t, \varrho) \tag{14}$$

is the vector of the unknown constants with $\overline{m}_{ij}$ the entries of $\overline{M}$, $\overline{p}_t = \overline{M}p_t$, and $\varrho = p_t^\top \overline{M}p_t$.

It is worth observing that estimating the constant vector $\mathrm{x}(x_t) \in \mathbb{R}^{10}$ is sufficient to obtain an estimate for $p_t$. Indeed, the first 6 components of $\mathrm{x}(x_t)$ give an estimate for $\overline{M}$ whereas $\overline{p}_t$ estimates $\overline{M}p_t$, so that $p_t$ can then be recovered by inversion of $\overline{M}$.

**Property 1** (Partial bijectivity of the map x)**.** *The map* $\mathrm{x} : \mathbb{R}^3 \times SO(3) \mapsto \mathbb{R}^{n_p}$ *is partially invertible with respect to $p_t$. There exists a partial left-inverse denoted* $\Upsilon$ *such that* $p_t = \Upsilon \circ \mathrm{x}(p_t, R_t)$ *for any* $(p_t, R_t) \in \mathbb{R}^3 \times SO(3)$ *and* $\Upsilon$ *is globally Lipschitz on* $\mathbb{R}^{10}$*, i.e. there exists a constant* $L > 0$ *such that, for any* $\mathrm{x}_1, \mathrm{x}_2 \in \mathbb{R}^{10}$, $\|\Upsilon(\mathrm{x}_1) - \Upsilon(\mathrm{x}_2)\| \leq L\|\mathrm{x}_1 - \mathrm{x}_2\|$.

In practice, such a global inverse of x can be obtained by projection of $\overline{M}$ in the following way. According to (10), $\overline{M}$ has as eigenvalues $\{a^2, a^2, b^2\}$. Therefore, given $\mathrm{x} \in \mathbb{R}^{10}$, denoting $\overline{M}$ and $\overline{p}_t$ the corresponding components, we can take $\Upsilon(\mathrm{x}) = \left(U\,\mathrm{sat}\,(\Sigma)\,V^\top\right)^{-1}\overline{p}_t$, where $U$, $\Sigma$ and $V^\top$ are the elements of the singular value decomposition of $\overline{M}$, such that $U\Sigma V^\top = \overline{M}$, and sat saturates the entries of the diagonal matrix $\Sigma$ in the interval $[\kappa^{-1}\min(a^2,b^2),\ \kappa\max(a^2,b^2)]$ where $\kappa \geq 1$ represents a tolerance factor.

*c) Noise model for the approximated ARVA:* Substituting the real noisy measurement $h_m$ in place of the ideal measurement $h_n$ in the definition of $\eta$ (12) leads to a new output defined by

$$y_t = \left(\frac{m}{\|h_m\|4\pi}\right)^{\frac{2}{3}}(ab)^2. \tag{15}$$

Now using a first order approximation on the noise ${}^r w$, we can write

$$y_t = \Phi^\top(p_r)\mathrm{x}(x_t) + \nu_t(p_r, x_t, t) \tag{16}$$

with

$$\nu_t(p_r, x_t, t) \approx (ab)^2 \frac{\partial}{\partial\, {}^r w}\left(\frac{m}{\|h_m\|4\pi}\right)^{\frac{2}{3}}\Bigg|_{{}^r w = 0} {}^r w(t). \tag{17}$$

**Property 2** (Source noise in $y_t$)**.** *There exists a class-$\mathcal{K}$ function $\gamma_t$ such that the output map $y_t$ of* (16) *verifies for all $t \geq 0$*

$$\|\nu_t(p_r, x_t, t)\| \leq \gamma_t(\|p\|).$$

A detailed analysis of the partial derivative in (17) reveals that $\gamma_t(\|p\|) = c\|p\|^5 \|{}^r w\|_\infty$ with $c > 0$ bounded. As consequence, the output $y_t$ becomes closer to $\Phi^\top(p_r)\mathrm{x}(x_t)$ (which is proportional to $\|p\|^2$) as $p$ get closer to zero (*i.e.* $p_r$ closer to $p_t$).

### C. Receiver dynamics

The dynamics of the receiver, in the inertial space, are captured by a model of the type [22]

$$\dot{x}_r = f_r(x_r, u) \quad , \quad y_r = x_r \tag{18}$$

with state $x_r = (p_r, v_r, R_r, {}^r\omega_r) \in \mathbb{R}^3 \times \mathbb{R}^3 \times SO(3) \times \mathbb{R}^3$ denoting the drones's position, velocity, orientation and angular velocity respectively, input $u \in \mathbb{R}^4_{>0}$ denoting the vector of the propeller speeds, and output $y_r = x_r$ fully known. For reasons of space, we omit to present the details on control design and we refer the interested reader to [22] where it is shown how, given a reference trajectory $\xi : \mathbb{R}_{\geq 0} \to \mathbb{R}^3$ that is twice differentiable with known first and second derivatives, and veryfying $\xi(t_0) = p_r(t_0)$, it is possible to design a high gain controller able to make $p_r$ track $\xi$.

### D. Overall system and problem statement

Gathering (16), (18) and the constant quantities $p_t$ and $R_t$, we finally get

$$\dot{x}_r = f_r(x_r, u) \quad , \quad \dot{x}_t = 0 \tag{19a}$$

with $x_t = (p_t, R_t) \in \mathbb{R}^3 \times SO(3)$, and outputs $y_t \in \mathbb{R}_{>0}$ and $y_r \in \mathbb{R}^3$ defined by

$$\begin{array}{rcl} y_t & = & \Phi^\top(p_r)\mathrm{x}(x_t) + \nu_t(p_r, x_t, t) \\ y_r & = & x_r \end{array} \tag{19b}$$

with the maps $\mathrm{x} : \mathbb{R}^3 \times SO(3) \to \mathbb{R}^{10}$ and $\Phi : \mathbb{R}^3 \to \mathbb{R}^{10}$ defined in (13) and (14). The goal is now to estimate the position $p_t$ of the victim as precisely as possible. We have seen that this reduces to the estimation of the constant $\mathrm{x}(x_t)$, whose observability is inherently linked to the invertibility of the known quantity $\Phi^\top(p_r)$ throughout time, namely its *persistence of excitation*. Due to the presence of the noise $\nu_t$, the problem can thus be cast as a robust observation problem of the partial state $p_r$ of (19a) from the measured output (19b).

## IV. Proposed Solution

Figure 2 depicts the proposed overall control scheme whose elements are detailed in the following sections.

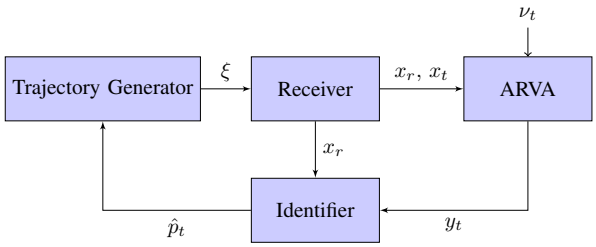


Fig. 2: Representation of the closed-loop system.

### A. Identifier

The role of the identifier is to provide an estimation of the victim position by properly processing the ARVA signal. This paper adopts the Recursive Least Square (RLS) with forgetting factor detailed in [14] and hereafter briefly recalled in its differential version. Given the ARVA measurement $y_t$ verifying (16), the RLS algorithm is given by:

$$\left\{ \begin{array}{rcl} \dot{R} & = & -\rho R + \dfrac{\phi\phi^\top}{1+\phi^\top\phi} \\ \dot{Q} & = & -\rho Q - \dfrac{\phi y_t}{1+\phi^\top\phi} \\ \dot{\hat{\mathrm{x}}} & = & -\Gamma\left(R\hat{\mathrm{x}} + Q\right) \end{array} \right. \quad , \quad \hat{p}_t = \Upsilon\left(\hat{\mathrm{x}}\right) \tag{20}$$

in which $\phi$ denotes the known signal $\Phi(p_r)$ of (16) to ease the reading, $\rho > 0$ represents the forgetting factor, the matrix $\Gamma = \Gamma^\top > 0$ is a scaling matrix, $R(0) = I$, and $Q(0) = 0$. If the vector $\Phi(p_r)$ is persistently exciting (see Definition 1) and in the ideal noise-free case where $y_t = \Phi(p_r)^\top \mathrm{x}(x_t)$, it has been demonstrated ([14]) that the origin of the estimation error $\hat{\mathrm{x}} - \mathrm{x}(x_t)$ is globally exponentially stable, and therefore $\lim_{t\to+\infty} \hat{p}_t(t) = p_t$. In presence of noise $\nu_t$ in (16) verifying Property 2, we can show the following.

**Property 3** (x-identifier)**.** *Assume Property 2 holds. Consider a signal $t \mapsto p_r(t)$ that is persistently exciting in the sense of Definition 1 for some $T$ and $\alpha_0$, and such that $\Phi(p_r)$ is bounded. For any identifier parameters $\rho > 0$ and $\Gamma = \Gamma^\top > 0$, there exist $\mu > 0$ and a class-$\mathcal{KL}$ function $\beta_p$ such that any trajectory $t \mapsto \hat{p}_t(t)$ of* (20) *satisfies*

$$\|\tilde{\mathrm{x}}(t)\| \leq \beta_p(\|\tilde{\mathrm{x}}(t_0)\|, t - t_0) + \mu\gamma_t(\|p\|_{t_0,t}) \tag{21}$$

*for all $t \geq t_0$, with $\tilde{\mathrm{x}} := \hat{\mathrm{x}} - \mathrm{x}(x_t)$ the estimation error.*

**Sketch of the proof.** From the excitation condition, $R(t) \geq \alpha_1 \mathrm{I}$ with $\alpha_1 = e^{-\rho T} \min\{\frac{\alpha_0 T}{1+\phi_m^2}, 1\}$ where $\phi_m$ bounds $\Phi(p_r)$. Then, taking $V(\tilde{\mathrm{x}}) = \dfrac{1}{2}\tilde{\mathrm{x}}^\top\Gamma^{-1}\tilde{\mathrm{x}}$ as candidate Lyapunov function, it turns out that $\dot{V} \leq -\alpha_1\|\tilde{\mathrm{x}}\|^2 + \dfrac{1}{2\rho}\|\tilde{\mathrm{x}}\|\gamma_t(\|p\|_{t_0,t}) + \mathrm{x}e^{-\rho(t-t_0)}\|\tilde{\mathrm{x}}\|$ which gives the ISS inequality (21) for a $\mu := (2\rho\alpha_1)^{-1}$.

### B. Reference Trajectory Generator

In order to use the identifier defined above, we need $\Phi(p_r)$ bounded and persistently exciting, and $p = p_r - p_t$ becoming sufficiently small to reduce the impact of the noise on the

estimation error $\tilde{\mathrm{x}}$. The idea is therefore to make $p_r$ follow a reference trajectory $\xi$ composed of an exciting part $\xi_e$ and a slow part $\xi_s$ steering $p_r$ to $p_t$, i.e. reducing $p$. Besides, in order to guarantee boundedness of trajectories, we saturate the slow component $\xi_s$ outside a bounded region where the victim is known to be. More precisely, the reference trajectory generator is represented by a dynamic system described by the following equations

$$\dot{\xi}_s = f_s(\hat{p}_t - \xi_s) \ , \quad \xi = \mathrm{sat}(\xi_s) + \xi_e \tag{22}$$

with $\xi_s(t_0) = p_r(t_0)$, $\xi_e(t) = \begin{pmatrix} A_1 \sin \varpi_1 t \\ A_2 \sin \varpi_2 t \\ A_3 \sin \varpi_3 t \end{pmatrix}$ and where $f_s(\cdot)$ is defined as

$$f_s(v) = f_{s_{\max}} \frac{K\|v\|}{\sqrt{1 + K^2\|v\|^2}} \frac{v}{\|v\|} \tag{23}$$

with $K > 0$. Notice that $f_s(\cdot)$ is continuous on $\mathbb{R}^3$, globally bounded by $f_{s_{max}}$ and such that $f(0) = 0$ and $f_s(v)$ has the direction of $v$. As said, the previous reference signal generator is justified by the "dual control" objective that characterizes the problem, namely exciting the system to identify the victim position and moving closer to the victim to have a better signal to noise ratio. The interplay between the two actions is managed by imposing two-time scales, which is enforced by reducing the parameter $f_{s_{max}}$. In fact, the following can be proved.

**Lemma 1.** *For any $A_i$, $\varpi_i$ defined as above, the signal $\xi_e$ is such that $\Phi(\xi_e)$ is bounded and PE, and there exists $f^\star_{s_{max}} > 0$ such that for all positive $f_{s_{max}} \leq f^\star_{s_{max}}$, $\Phi(\xi_e + \mathrm{sat}(\xi_s))$ is also bounded and PE.*

The proof is omitted due to space constraints.

## V. Main result

We now analyse the stability of the interconnection between the identifier (20) and the reference trajectory (22). The following theorem claims that if the time scales of the references $\xi_e$ and $\xi_s$ are sufficiently different (namely if $f_{s_{max}}$ is taken sufficiently small in relation to the $\varpi_i$), then the estimate of the victim position practically converges to zero with a practical region that is affected by the amplitude of the exciting signal. Such property, indeed, holds as long as the receiver remains sufficiently close to the victim in relation to the noise features.

**Theorem 1.** *Let parameters $\varpi_i$, $A_i$, $\rho$, $\Gamma$ be defined as in the previous sections. There exists $f^\star_{s_{max}} > 0$ such that for all positive $f_{s_{max}} \leq f^\star_{s_{max}}$ there exists a class-$\mathcal{K}$ function $\gamma$ such that any trajectory of* (19) *verifying $p_r \equiv \xi$ with $\xi$ the reference trajectory defined by* (20)*,* (22) *gives*

$$\limsup_{t\to\infty} \|p_r - p_t\| + \|\hat{p}_t - p_t\| \leq \gamma(\|\xi_e\|_\infty)$$

*as long as $p_r \in \mathcal{B}_{\rho^\star}(p_t)$, with $\rho^\star = \left(\dfrac{1}{c\mu L \|{}^r w\|_\infty}\right)^{\frac{1}{4}}$.*

We observe that, due to the persistent excitation, we cannot ensure $p_r = p_t$ asymptotically, and from Property 2, the noise $\nu_t$ does not completely disappear, producing a residual error on the estimation depending on the size of $\gamma_t$.

The size of the region $\mathcal{B}_{\rho^\star}(p_t)$ which guarantees stability and nice asymptotic properties increases when either the amplitude of the noise $\|{}^r w\|_\infty$ or the parameter $\mu$ decrease. But, according to Property 3, reducing $A_i$ reduces the asymptotic effect of the noise ${}^r w$ on the estimation error $\tilde{\mathrm{x}}$, so that, unfortunately, a reduction of the amplitudes $A_i$ leads both to a reduction of the asymptotic norm of $\tilde{\mathrm{x}}$ and to a reduction of the stability domain. So, there exists a design compromise between the stability requirement and the asymptotic performance.

## VI. Simulation results

The simulator is implemented following the scheme of Figure 2 whose blocks have been implemented in a Matlab® Simulink® model. The simulator solver has been set to integrate the continuous time ordinary differential equations with an explicit $4^{\text{th}}$ order solver (ode45 Dormand-Prince), exploiting a variable step size upper bounded by 1 ms. Furthermore, the algorithm implementation into the UAV flight control unit (PixHawk) has been tested in a dedicated software-in-the-loop system, also comprehensive of the ARVA simulator, submitted to the Springer Book Robot Operating System, Volume 5. The ARVA noise, ${}^r w(t)$, has been defined as a randomly oriented vector whose magnitude and attitude are generated by means of band-limited withe noise blocks. In particular, the magnitude of the noise is bounded by $\|{}^r w\|_\infty \leq \bar{w} := (2\pi\|p_{\text{eq}}\|^3)^{-1}$ with $\|p_{\text{eq}}\| = 80$ meters. This value has been identified after a field test campaign that was performed by measuring the relative position of the receiver with respect to the transmitter (by means of GPS receivers), their relative attitude (by means of Inertial Measurement Units) and the ARVA data. The maximum environment induced EMI are estimated to be equivalent to an ARVA signal emitted by a transmitter approximately located 80 meters far from the receiver. The relevant control parameters are $K = 1$ and $f_{s_{\max}} = 0.5$ m/s whereas the RLS algorithm is characterized by the forgetting factor $\rho = 1$. The excitation trajectory $\xi_e = \mathrm{col}(\xi_{e_1}, \xi_{e_2}, \xi_{e_3})$ is designed with $\xi_{e_i} = A_i \sin(\omega_i t)$, $i = 1, 2, 3$ with $A_1 = A_2 = A_3 = 2$ m and $\omega_1 = 0.7\,2\pi$, $\omega_2 = \omega_1/2$ and $\omega_3 = \omega_1/4$ rad/s. The parameters of the reference trajectory, $f_{s_{\max}}$, $A_i$ and $\omega_i$, have been chosen in agreement with the limitations on the maximum speed of 6 m/s that the quad-copters under development in the Airborne project will have in avalanche operations. The simulations assume that the centre of the inertial reference system (which is defined by the user) coincides with the initial position of the drone, *i.e.* $p_r(0) = 0$. At time $t = 0$ also the reference trajectory $\xi_s$ is set to be null, thus leading to $\xi_s(0) = 0$, whereas the position of the transmitter is randomly generated to belong to a sphere of radius equal to 50 m, centred at the origin of the inertial space. The maximum initial distance of 50 m has been selected on the base of practical experiments which validated the maximum ratings declared in the data-sheets of the most famous ARVA devices [23], [24]. It is worth noting that, for longer distances the ARVA signal-to-noise ratio would be too small for letting the algorithm working properly. In particular, the simulations are obtained with

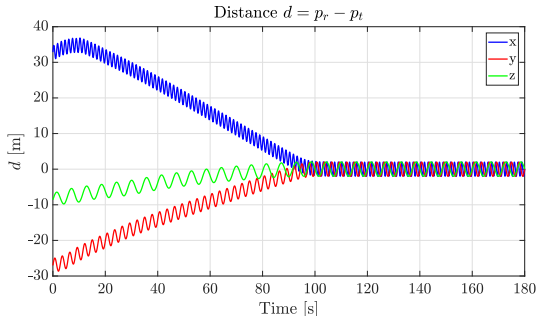


Fig. 3: Distance $d$ from the transmitter to the receiver

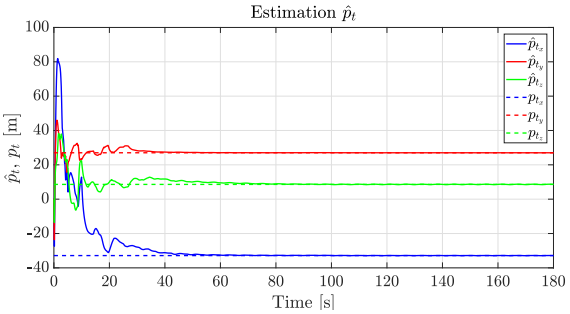


Fig. 4: Estimate of the victim position $\hat{p}_t$.

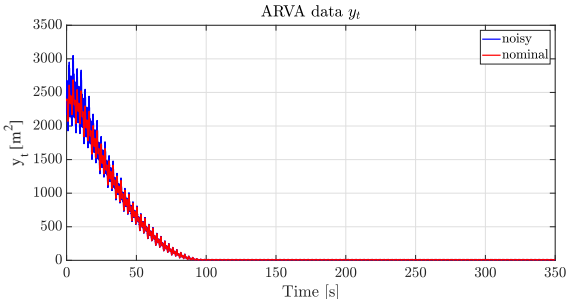


Fig. 5: Effect of the noise $\nu_t$ on the ARVA data

$p_t = \text{col}(-32.8, 27.0, 8.6)$ m.

Figure 3 depicts the trajectory of the receiver with respect to the transmitter and Figure 4 the estimation $\hat{p}_t$. The initial estimation is poor due to the long relative distance from the receiver to the transmitter which makes the ARVA data particularly noisy. After about 10 seconds, the identifier collects data rich enough to estimate more accurately the transmitter position. Due to the double time scale (guaranteed by small $f_{s_{\max}}$) between the identifier (faster) and the reference trajectory (slower), the receiver is slowly driven toward the estimated transmitter position which rapidly converges to the right value. On the other hand, the estimation gets more and more accurate as far as the receiver is close to the transmitter. Indeed, in Figure 5 the nominal ARVA output is superposed to the noisy one. We observe that the noise disappear as the receiver approaches the transmitter. It is important to note that a reliable estimate of the victim's position is obtained before the receiver reaches the victim, which constitutes a significant advantage with respect to extremum-seeking techniques.

The choice of $f_{s_{\max}}$ influences the stability of the overall control scheme (in agreement with the theoretical result). In particular, Figures 6-7 depict how the trajectories of the estimation error $\tilde{p}_t$ and the distance $\xi_s - p_t$ change with respect to the variation of $f_{s_{\max}}$. A reduction of $f_{s_{\max}}$ leads to a more conservative satisfaction of the stability criterion but makes the receiver staying longer in the noisier zone. As consequence, the estimation of the transmitter position provided by the identifier is less accurate. Vice-versa, higher values of $f_{s_{\max}}$ induce the receiver to move faster toward the less noisy zone but satisfy in a less conservative way the stability. For this reason, the parameter $f_{s_{\max}}$ is subject to a design compromise between stability and performance.

## VII. Conclusions and Future Works

This paper presented an identification scheme solving the problem of automatic estimation of the position of avalanche victims who wear a special device called ARVA transmitter. Due to the peculiar properties of the output map associated to the ARVA receiver, the identification process provided by the simple implementation of a recursive least square algorithm does not provide the best performance if not supported by a control system which steers the receiver toward the transmitter. The effectiveness of the proposed control scheme was tested in simulations. Future works will regard the real implementation of the proposed strategy on the drones developed in the AirBorne European project (targeting a TRL8 aerial platform).

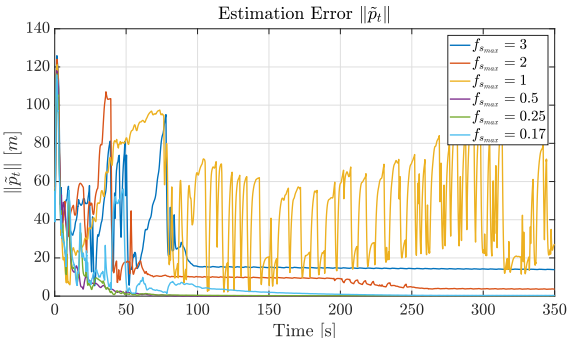


Fig. 6: Comparison of the estimation error $\tilde{p}_t$ with different values of $f_{s_{\max}}$.

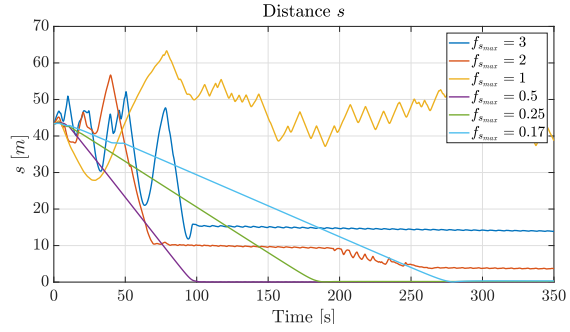


Fig. 7: Comparison of the distance $s = \xi_s - p_t$ with different values of $f_{s_{\max}}$.

## REFERENCES


[1] J. Cacace, A. Finzi, V. Lippiello, M. Furci, N. Mimmo, and L. Marconi, "A control architecture for multiple drones operated via multimodal interaction in search & rescue mission," in *2016 IEEE International Symposium on Safety, Security, and Rescue Robotics (SSRR)*. IEEE, 2016, pp. 233–239.

[2] J. Cacace, A. Finzi, and V. Lippiello, "Implicit robot selection for human multi-robot interaction in search and rescue missions," in *2016 25th IEEE International Symposium on Robot and Human Interactive Communication (RO-MAN)*. IEEE, 2016, pp. 803–808.

[3] G. Bevacqua, J. Cacace, A. Finzi, and V. Lippiello, "Mixed-initiative planning and execution for multiple drones in search and rescue missions," in *Twenty-Fifth International Conference on Automated Planning and Scheduling*, 2015.

[4] L. Marconi, C. Melchiorri, M. Beetz, D. Pangercic, R. Siegwart, S. Leutenegger, R. Carloni, S. Stramigioli, H. Bruyninckx, P. Doherty *et al.*, "The sherpa project: Smart collaboration between humans and ground-aerial robots for improving rescuing activities in alpine environments," in *2012 IEEE International Symposium on Safety, Security, and Rescue Robotics (SSRR)*. IEEE, 2012, pp. 1–4.

[5] AerIal RoBotic technologies for professiOnal seaRch aNd rescuE. [Online]. Available: https://www.airborne-project.eu/

[6] E. Bregu, N. Casamassima, D. Cantoni, L. Mottola, and K. Whitehouse, "Reactive control of autonomous drones," in *Proceedings of the 14th Annual International Conference on Mobile Systems, Applications, and Services*. ACM, 2016, pp. 207–219.

[7] M. Silvagni, A. Tonoli, E. Zenerino, and M. Chiaberge, "Multipurpose uav for search and rescue operations in mountain avalanche events," *Geomatics, Natural Hazards and Risk*, vol. 8, no. 1, pp. 18–33, 2017.

[8] M. Grauwiler and L. Oth, "Alcedo–the flying avalanche transceiver," *Zurich: European Satellite Navigation Competition*, 2010.

[9] J. Cochran and M. Krstic, "Source seeking with a nonholonomic unicycle without position measurements and with tuning of angular velocity part i: Stability analysis," in *2007 46th IEEE Conference on Decision and Control*. IEEE, 2007, pp. 6009–6016.

[10] J. Cochran, A. Siranosian, N. Ghods, and M. Krstic, "Source seeking with a nonholonomic unicycle without position measurements and with tuning of angular velocitypart ii: Applications," in *2007 46th IEEE Conference on Decision and Control*. IEEE, 2007, pp. 1951–1956.

[11] J. Cochran, N. Ghods, and M. Krstic, "3d nonholonomic source seeking without position measurement," in *2008 American Control Conference*. IEEE, 2008, pp. 3518–3523.

[12] C. G. Mayhew, R. G. Sanfelice, and A. R. Teel, "Robust source-seeking hybrid controllers for nonholonomic vehicles," in *2008 American Control Conference*. IEEE, 2008, pp. 2722–2727.

[13] C. Mellucci, P. P. Menon, C. Edwards, and P. Challenor, "Source seeking using a single autonomous vehicle," in *2016 American Control Conference (ACC)*. IEEE, 2016, pp. 6441–6446.

[14] P. A. Ioannou and J. Sun, *Robust adaptive control*. Courier Corporation, 2012.

[15] R. Mehra, "Optimal input signals for parameter estimation in dynamic systems–survey and new results," *IEEE Transactions on Automatic Control*, vol. 19, no. 6, pp. 753–768, 1974.

[16] V. V. Fedorov, *Theory of optimal experiments*. Elsevier, 2013.

[17] G. C. Goodwin and R. L. Payne, *Dynamic system identification: experiment design and data analysis*. Academic press, 1977.

[18] M. Zarrop, "Optimal experiment design for dynamic system identification," *Lecture Notes in Control and Information Sciences*, vol. 21, 1979.

[19] P. Piniés and J. D. Tardós, "Fast localization of avalanche victims using sum of gaussians," in *Proceedings 2006 IEEE International Conference on Robotics and Automation, 2006. ICRA 2006.* IEEE, 2006, pp. 3989–3994.

[20] K. Reif, F. Sonnemann, and R. Unbehauen, "An ekf-based nonlinear observer with a prescribed degree of stability," *Automatica*, vol. 34, no. 9, pp. 1119–1123, 1998.

[21] G. Besançon, *Nonlinear observers and applications*. Springer, 2007, vol. 363.

[22] R. Naldi, M. Furci, R. G. Sanfelice, and L. Marconi, "Robust global trajectory tracking for underactuated vtol aerial vehicles using inner-outer loop control paradigms," *IEEE Transactions on Automatic Control*, vol. 62, no. 1, pp. 97–112, 2016.

[23] Ortovox, "Arva ortovox 3+ user manual," May 2019.

[24] Barryvox, "Arva mammut barryvox user manual," May 2019.